Multiple Scattering of Neutrons in Vanadium and Copper

I. A. BLECH AND B. L. AVERBACH
Department of Metallurgy, Massachusetts Institute of Technology, Cambridge, Massachusetts
(Received 18 September 1964)

The intensity of multiply scattered neutrons from cylindrical specimens of incoherent isotropic scatterers has been calculated and compared with experimental values. The scattering is considered in terms of the number of scattering events, and the intensity is expressed in terms of the parameters μR, R/h, and σ_s/σ_t, where μ is the absorption coefficient, R is the radius, h is the height of the cylinder, σ_s is the scattering cross section, and σ_t is the total cross section. Intensities were measured as a function of R/h for vanadium, which scatters almost entirely incoherently, and for copper, which has strong coherent reflections. The data for vanadium and copper are in good agreement with the calculations.

I. INTRODUCTION

IT is frequently necessary to separate the primary scattering of neutrons from the secondary and subsequent orders of scattering in interpreting measurements of diffuse intensities. This is particularly important in the case of vanadium, since it is frequently used to standardize incoherent scattering. The multiple scattering correction is also important in studies of magnetic and temperature diffuse scattering, since it may represent a substantial portion of the diffuse intensity. The problem of multiple scattering events has been treated in a general way,[1] and a solution for the multiple scattering of neutrons by infinite slabs of an isotropic scatterer has been derived by Vineyard.[2]

The latter calculation separates the primary scattering in which neutrons have suffered only one diffraction event, from the second order, where two diffraction events have occurred, and finally from all subsequent higher order events. Vineyard calculated the second order scattering and then estimated the total multiple scattering. Brockhouse *et al.*[3] compared these calculations with data obtained with several coherent scatterers and found this quasiisotropic approximation to give reasonably good agreement.

We have followed the same approach used by Vineyard for the case of cylindrical samples completely bathed in a homogeneous neutron beam. The problem involves a series of definite integrals which yield the successive orders of scattering for an incoherent isotropic scatterer, neglecting inelastic effects. The secondary scattering was evaluated numerically by means of a machine calculation. The multiple scattering is a function of μR, R/h, and σ_s/σ_t, and the calculation was tested by a comparison with data obtained from specimens with various values of R/h. These specimens were made up of a series of discs separated by cadmium spacers. In the case of vanadium, the calculations are in good agreement with the measurements. In the case of copper, which has strong coherent reflections, it appears that the calculation underestimates the multiple scattering from tall cylinders. The absolute values of the multiple scattering are significant; for vanadium the multiple scattering was up to about 25% of the measured total diffuse scattering, and for copper it was up to 85% of the measured diffuse scattering.

II. CALCULATION OF MULTIPLE SCATTERING

The number of neutrons per unit solid angle scattered in a primary fashion from a unit volume dV for an incoming flux J_0 is given by

$$dI_1=\frac{1}{4\pi}(N_V\sigma_s J_0)e^{-\mu L_I}dV. \tag{1}$$

Here, dI_1 is the number of primary scattered neutrons per unit solid angle, N_V the atomic density in atoms/cm^3, σ_s the scattering cross section, μ the total absorption, and L_I is the path length of the incoming beam as shown in Fig. 1. The total primary scattering I_1 in neutrons per solid angle is then

$$I_1=\int_V e^{-\mu L_{II}}dI_1, \tag{2}$$

where L_{II} is the path length of the scattered beam (Fig. 1). The secondary intensity from a volume element

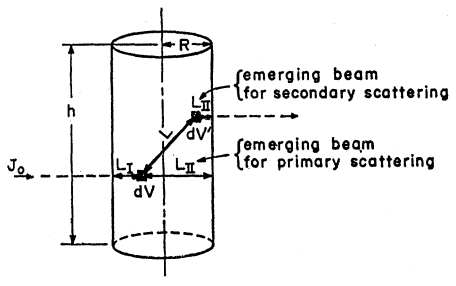

FIG. 1. Primary and secondary scattering.

[1] S. Chandrasekhar, *Radiative Transfer* (Clarendon Press, Oxford, England, 1950); S. Chandrasekhar, D. Elbert, and A. Franklin, Astrophys. J. **115**, 244 (1952).
[2] G. H. Vineyard, Phys. Rev. **96**, 93 (1954).
[3] B. N. Brockhouse, L. M. Corliss, and J. M. Hastings, Phys. Rev. **98**, 1721 (1955).

dV' can now be calculated from the primary scattering,

$$dI_2=\left\{N_V\sigma_s\int_V\frac{dI_1}{4\pi L^2}e^{-\mu L}dV\right\}dV' \tag{3}$$

and the total secondary intensity I_2 becomes

$$I_2=\int_V e^{-\mu L_{II}}dI_2. \tag{4}$$

Similarly, the nth order scattering will be

$$I_n=\int_V e^{-\mu L_{II}}dI_n, \tag{5}$$

where

$$dI_n=\left\{N_V\sigma_s\int_V\frac{dI_{n-1}}{4\pi L^2}e^{-\mu L}dV\right\}dV'. \tag{6}$$

The total scattering (in neutrons/steradian) is the sum of all of the orders of scattering,

$$I=I_1+I_2+I_3+\cdots=\sum_{n=1}I_n. \tag{7}$$

Assuming $I_n/I_{n-1}=I_2/I_1=\delta'$, $n=2, 3,\cdots n$, the multiple scattering I_m is

$$I_m=I-I_1=I_2+I_3+\cdots=I_1(\delta'/1-\delta'). \tag{8}$$

Equation (8) is expected to hold whenever I_2/I_1 is appreciably smaller than unity.

We now take up the calculation of the ratio of the secondary to primary scattering, δ'. Combining Eqs. (1)–(4) gives

$$I_2=\frac{1}{4\pi}(N_V{}^2\sigma_s{}^2J_0)\int_{V'}\int_V\frac{e^{-\mu L}}{4\pi L^2}e^{-\mu(L_I+L_{II})}dVdV' \tag{9}$$

and

$$I_1=\frac{1}{4\pi}(N_V\sigma_sJ_0)\int_V e^{-\mu(L_I+L_{II})}dV. \tag{10}$$

The ratio δ' becomes

$$\delta'=\frac{I_2}{I_1}=\frac{N_V\sigma_s}{\mu}\delta=\left(\frac{\sigma_s}{\sigma_t}\right)\delta, \tag{11}$$

where σ_t is the total cross section (scattering and absorption) and

$$\delta=\mu\int_V\int_{V'}(e^{-\mu L}/4\pi L^2)\times e^{-\mu(L_I+L_{II})}dVdV'\Big/\int_V e^{-\mu(L_I+L_{II})}dV. \tag{12}$$

The denominator of Eq. (12) is recognized to be the cylindrical attenuation factor $A(\theta)$, which is tabulated elsewhere,[4] multiplied by the specimen volume V. The numerator has to be integrated twice over the specimen volume. It is convenient to rewrite Eq. (12) in terms of the cylindrical coordinate systems shown in Fig. 2. The resulting equation is

$$\delta=\frac{\mu}{A(\theta)}\left(\frac{2}{4\pi^2R^2h}\right)\int_{r=0}^{R}\int_{r'=0}^{R}\int_{\theta=0}^{2\pi}\int_{\theta'=0}^{2\pi}\int_{Z=0}^{h}\int_{Z'=0}^{h-Z}\frac{e^{-\mu L}}{L^2}\times e^{-\mu(L_I+L_{II})}rr'drdr'd\theta d\theta'dZdZ', \tag{13}$$

where R and h are the specimen radius and height, respectively. The quantities r, θ, Z, r', θ', Z' are the cylindrical coordinates. From Fig. 2 it is evident that

$$L^2=Z'^2+r^2+r'^2-2rr'\cos(\theta-\theta'). \tag{14}$$

The factor δ was obtained by means of a numerical calculation of Eq. (13) using the integration outlined in the Appendix. These values are tabulated in Table I as a function of μR for different values of R/h. Figure 3 shows that δ can be quite large for small values of R/h. It is also interesting to note (Appendix) that δ is approximately independent of scattering angles at small values of μR and at small angles. The secondary scattering can be readily calculated from

$$\sigma_2=\sigma_1(\sigma_s/\sigma_t)\delta, \tag{15}$$

where σ_1 and σ_2 are the differential cross sections for primary and secondary scattering, and the multiple

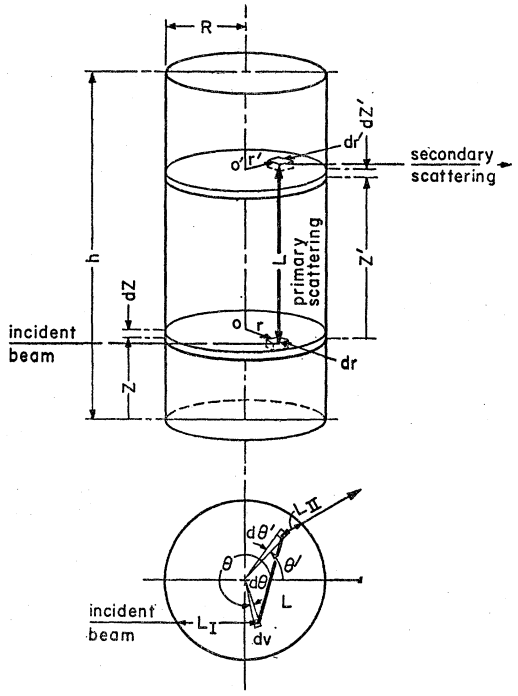

FIG. 2. Secondary scattering in cylindrical samples.

[4] *International Tables for X-Ray Crystallography* (The Kynoch Press, Birmingham, England, 1962), Vol. II.

TABLE I. Coefficient δ for secondary scattering.

	μR								
R/h	0.1	0.2	0.3	0.4	0.5	0.6	0.7	0.8	0.9
0.10	0.1049	0.1922	0.2657	0.3286					
0.12	0.1023	0.1878	0.2600	0.3212	0.2742				
0.14	0.1001	0.1841	0.2553	0.3157	0.3670	0.4118			
0.16	0.0981	0.1809	0.2512	0.3110	0.3616	0.4046	0.4422		
0.18	0.0963	0.1780	0.2475	0.3067	0.3570	0.3933	0.4349	0.4661	
0.20	0.0946	0.1752	0.2440	0.3028	0.3527	0.3947	0.4295	0.4585	
0.22	0.0931	0.1726	0.2407	0.2991	0.3488	0.3905	0.4250	0.4530	0.4751
0.24	0.0916	0.1701	0.2376	0.2955	0.3450	0.3866	0.4210	0.4486	0.4701
0.26	0.0902	0.1677	0.2345	0.2921	0.3413	0.2829	0.4172	0.4447	0.4657
0.28	0.0888	0.1654	0.2316	0.2887	0.3377	0.3792	0.4136	0.4411	0.4619
0.30	0.0895	0.1631	0.2287	0.2854	0.3342	0.3756	0.4100	0.4376	0.4586
0.40	0.0819	0.1536	0.2165	0.2715	0.3193	0.3605	0.3953	0.4239	0.4461
0.50	0.0768	0.1445	0.2044	0.2573	0.3036	0.3439	0.3785	0.4073	0.4303
1.00	0.0615	0.1174	0.1682	0.2143	0.2560	0.2937	0.3273	0.3571	0.3830
2.00	0.0425	0.0818	0.1181	0.1516	0.1825	0.2110	0.2370	0.2607	0.2820
3.00	0.0333	0.0644	0.0933	0.1203	0.1454	0.1687	0.1904	0.2103	0.2286
4.00	0.0277	0.0535	0.0778	0.1005	0.1218	0.1418	0.1604	0.1776	0.1936
5.00	0.0237	0.0460	0.0670	0.0867	0.1053	0.1227	0.1391	0.1543	0.1685

scattering cross section σ_m,

$$\sigma_m=\frac{\sigma_s(\sigma_s/\sigma_t)\delta}{1-(\sigma_s/\sigma_t)\delta}, \tag{16}$$

where σ_s is the total scattering cross section.

III. EXPERIMENTAL CORRELATION

Vanadium has a very small coherent cross section and may be regarded as an isotropic incoherent scatterer. This material is thus well suited for a test of the calculations. Stacks of disks of 1.9-cm diameter and different heights were used. Cadmium spacers, 0.030 cm thick, were used to absorb the neutrons traveling between the disks. Five sets of cylinders, ranging from one solid cylinder to one containing 17 layers, were used. This experimental arrangement provided comparable scattering intensities for a variety of values of R/h. The observed intensities were corrected for the volume occupied by the spacers.

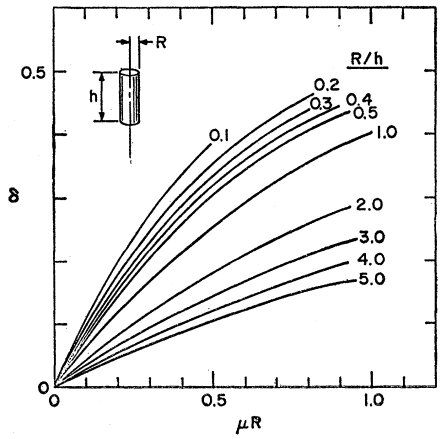

FIG. 3. Coefficient of secondary scattering.

A lead monochromator arranged to provide a neutron beam of 1.20 Å was used, and a BF_3 counter was mounted on the spectrometer. Experiments were carried out with a roughly collimated incoming beam and a collimator in front of the counter. Measurements were repeated without the scatter collimator, and also with a collimator in front of the specimen to minimize the vertical divergence of the entering beam. These variations in collimation made little difference in the results. The usual background corrections were made and standardization was accomplished by comparison with the (111), (200), and (220) peaks from nickel powder. The measured cross sections for vanadium at a scattering angle (2θ) of 20° are shown as a function of the specimen height in Fig. 4, and these agree well with the values

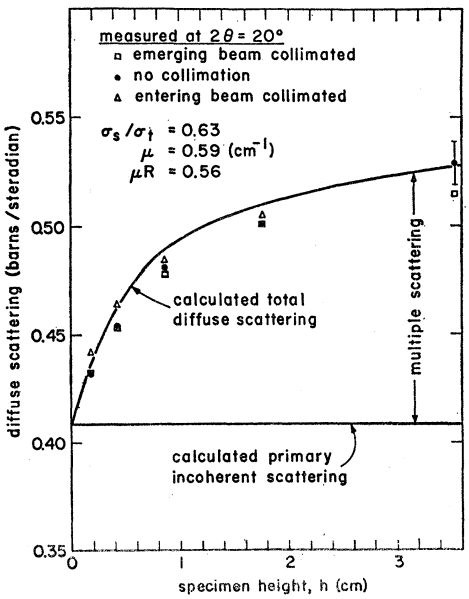

FIG. 4. Diffuse scattering of vanadium cylinders.

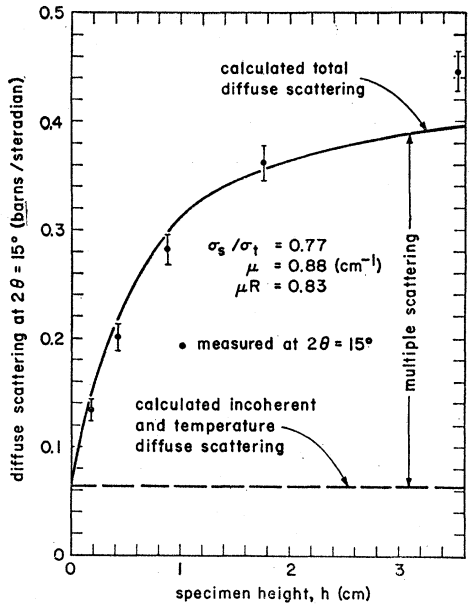

FIG. 5. Diffuse scattering of polycrystalline copper.

calculated from Eq. (16). The multiple scattering in a vanadium cylinder 3.5 cm high and 1.9 cm in diameter is about 0.12 b/sr. This is about 25% of the measured total diffuse scattering, and it is evident that the multiple scattering cannot be ignored if sizeable specimens are used.

The diffuse scattering cross section for polycrystalline copper was measured near the (111) peak. Copper has strong coherent peaks, and the results shown in Fig. 5 show that the multiple scattering is also large. The analysis given above holds well at small values of R/h, but the multiple scattering for tall specimens is underestimated. Up to about 85% of the observed diffuse scattering arises from multiple scattering.

These data indicate that Eq. (8) provides a useful expression for the multiple scattering of cylindrical specimens.

ACKNOWLEDGMENTS

The authors would like to acknowledge the support of the National Science Foundation and the assistance of the MIT Computation Center. The numerous discussions with Professor C. G. Shull were also very helpful.

APPENDIX

Evaluation of the Secondary Scattering Coefficient δ

The attenuation along L_{I} and L_{II} was assumed to be the same as for the primary scattering. Thus, Eq. (13) becomes

$$\delta=\frac{\mu}{2\pi^2R^2h}\int_{r=0}^{R}\int_{r'=0}^{R}\int_{\theta=0}^{2\pi}\int_{\theta'=0}^{2\pi}\int_{Z=0}^{h}\int_{Z'=0}^{h-Z}\frac{e^{-\mu L}}{L^2}\times rr'drdr'd\theta d\theta'dZdZ'. \quad (17)$$

Next we redefine θ as $\theta-\theta'$, and integrate Eq. (16) to get

$$\delta=\frac{2\mu}{\pi R^2h}\int_{r=0}^{R}\int_{r'=0}^{R}\int_{\theta=0}^{\pi}\int_{Z=0}^{h}\int_{Z'=0}^{h-Z}\frac{e^{-\mu L}}{L^2}\times rr'drdr'd\theta d\theta'dZdZ' \quad (18)$$

and

$$L^2=Z'^2+r^2+r'^2-2rr'\cos\theta.$$

It is convenient to treat the last integral in terms of dimensionless variables, $\eta=r/h$, $\eta'=r'/h$, $\zeta=Z/h$, $\zeta'=Z'/h$, $N=R/h$, and $M=\mu R$. Expanding the integrand in series leads to

$$\delta=\left(\frac{2}{\pi N^3}\right)\sum_{i=0}^{\infty}\frac{M^{i+1}}{i!N^i}\times\int_{\eta=0}^{N}\int_{\eta'=0}^{N}\int_{\theta=0}^{\pi}\langle dI(i)\rangle\eta\eta'dyd y'd\theta, \quad (19)$$

where

$$dI(i)=\int_{\zeta=0}^{1}\int_{\zeta'=0}^{1-\zeta}(-1)^i(L')^{i-2}d\zeta d\zeta' \quad (20)$$

$$L'^2=\zeta'^2+\eta^2+\eta'^2-2\eta\eta'\cos\theta.$$

The integrands in Eq. (19) can be readily calculated from Eq. (20), and dI_0 through dI_6 were assessed in this manner. The integration in Eq. (19) has been carried out numerically using a digital computer IBM 7094, and the results are tabulated in Table I.

Equation (19) was also integrated with the factor $e^{-\mu(L_{\mathrm{I}}+L_{\mathrm{II}})}$ in the integrand to test the first assumption. The results indicate that even at $\mu R=0.8$ and at scattering angles between 0° and 30°, the assumption is good within 1%.